Phase evolution during the low temperature formation of calcium-deficient hydroxyapatite–gypsum composites

Yaser E. Greish *

Department of Chemistry, College of Science, United Arab Emirates University, Al Ain, P.O. Box 17551, United Arab Emirates

Abstract

Calcium-deficient hydroxyapatite is known to have a closer similarity to bone structure than the stoichiometric version, and is therefore used in bone cement applications. Both Ca-def apatite and plaster of Paris ($CaSO_4 \cdot 1/2H_2O$, POP) are known as bioresorbable bone cements. The current study investigated the formation of composites involving POP with each of three types of Ca-def apatites (abbreviated as CDS, CDH, and S-CH) with Ca/P molar ratios of 1.5–1.6. The kinetics, variations in solution chemistry during the formation of these composites and phase compositions of the formed products were investigated over a course of 24 h. All types of Ca-def apatites caused a delay of the growth kinetics of gypsum with different extents. The release of Ca^{2+} and PO_4^{3-} ions from the apatites is believed to be the main reasons for such a retardation effect. Moreover, the presence of gypsum precursors was shown to decrease the alkalinity of the medium involving CDS formation and to buffer the medium involving the formation of CDH and S-CH from their precursors.
© 2011 Published by Elsevier Ltd and Techna Group S.r.l.

Keywords: Gypsum; Calcium-deficient hydroxyapatite; Isothermal calorimetry; Phase composition; Microstructure

1. Introduction

The mineral component of all hard tissues is known as hydroxyapatite. Combined with the fibrous collagen, hard tissues are known for their unique properties. Stoichiometric hydroxyapatite (SHAp, $Ca_{10}(PO_4)_6(OH)_2$) is frequently regarded as a model for bone mineral. The Ca/P molar ratio of this composition is 1.67. HAp, however, is not a compound of fixed composition and can incorporate many substituents either in the Ca^{2+} sites, the PO_4^{3-} sites, the OH^- sites or combinations of all sites [1]. These substitutions affect the Ca/P molar ratio [2]. A general compositional formula was, therefore, considered for non-substituted calcium-deficient HAp as $Ca_{10-x}(HPO_4)_x(PO_4)_{6-x}(OH)_{2-x}$, where x ranges from 0 to 1 [3]. In particular, the ratio of Ca/P in HAp can vary between the compositional limits of about 1.5 and 1.67. At Ca/P ratios below 1.67, HAp is known as calcium-deficient apatite. The extent of calcium deficiency affects the stability of HAp, increases its bioactivity, and increases its

solubility product [4]. These properties have led to the classification of Ca-def apatites as bioresorbable materials. Resorption of these apatites takes place in the body after implantation in a process called "remodeling" where the implanted Ca-def apatite dissolves and re-precipitates in the form of bone-like apatite. These Ca-def apatites are, therefore, preferable to be used as bone cements in sites where formation of new bone is required. Compared with calcium phosphates that are prepared at high temperatures, Ca-def apatites prepared as injectable cements at low temperatures have received a lot of attention for its convenience and ease of preparation [5]. They are ideal as reconstructive materials for bone defects, they fit in well, harden *in situ*, and are replaced by osseous tissues [6]. Ca-def apatites formed by cement-type reaction were previously studied [7,8]. Starting materials were single phase α-tricalcium phosphate (α-$Ca_3(PO_4)_2$; α-TCP) or a combination of acidic dicalcium phosphate ($CaHPO_4 \cdot 2H_2O$; DCPD or $CaHPO_4$; DCPA) and basic tetracalcium phosphate ($Ca_4(PO_4)_2O$; TetCP). Hydration in each case leads to the formation of Ca-def apatite. However, using α-TCP, as a single component bone cement, may require lengthy periods for complete reaction to occur [7]. On the other hand, formulations involving TetCP and DCPA (or DCPD) were shown to have better kinetics of apatite formation upon hydration 5–8.

* Corresponding author. Permanent address: Department of Ceramics, National Research Centre, Cairo, Egypt. Tel.: +971 50 2338203; fax: +971 3 7671291.

E-mail address: y.afifi@uaeu.ac.ae.

Moreover, it has been shown to provide flexibility for controlling the calcium deficiency in the produced apatite [8].

Gypsum ($CaSO_4 \cdot 2H_2O$), on the other hand, is a highly biocompatible material that is one of the simplest synthetic bone graft materials with the longest clinical history, spanning more than 100 years [9]. It is classified as a bioresorbable material. It has been successfully used to treat periodontal diseases, endodontic lesions, alveolar bone loss, and for maxillary sinus augmentation [9]. It has been also used as a binder to facilitate healing and prevent loss of the grafting material. Moreover, it is tissue compatible, and does not interfere with the healing process [10]. Gypsum is formed through the hydration of its precursor; plaster of Paris ($CaSO_4 \cdot 0.5H_2O$; POP), according to reaction (1):

$$CaSO_4 \cdot 0.5H_2O + 1.5H_2O \rightarrow CaSO_4 \cdot 2H_2O \qquad (1)$$
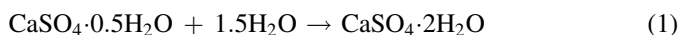
Combinations of POP and calcium phosphates have been previously investigated [11–19]. Due to its relatively faster setting process, POP was added to improve the setting reactions of a biodegradable calcium phosphate cement that was composed of β-tricalcium phosphate (β-$Ca_3(PO_4)_2$; β-TCP) and monocalcium phosphate monohydrate ($Ca(H_2PO_4)_2 \cdot H_2O$; MCPM) [12]. These cement composites were proven to be osteoconductive [12]. POP was also used to modulate the setting time, workability and porosity of a cement composed of an aqueous slurry of α-TCP [13–15]. Nilsson et al. [14] realized the major role of gypsum when it was mixed with α-TCP where it helped in the creation of pores in the implanted material, thus ensuring ingrowth of new bone tissue. In addition, POP-based biomaterials have also exhibited promise as grafts in a preclinical repair model of intrabony periodontal defects, as well as in clinical reports for sinus augmentation and treatments of femoral shaft non-unions [16–18]. Combinations of ready-made HAp particles with gypsum were also evaluated. Sato et al. indicated the promising characteristics of gypsum after mixing it with HAp particles, based on the relatively fast absorption of gypsum without interfering with the process of bone healing [19]. The current study investigates the effect of adding Ca-def apatites with different origins and Ca/P molar ratios on the chemistry of formation and growth kinetics of gypsum in their composites.

2. Materials and methods

The different types of Ca-deficient hydroxyapatites used in the current study included a synthetic hydroxyapatite, and two cement-type apatites. Synthetic Ca-def apatite, abbreviated hereafter as S-CH had a Ca/P molar ratio of 1.6 and was prepared by a common wet method. A 0.3 M aqueous solution of $NH_4H_2PO_4$ (obtained from Sigma–Aldrich, USA) was added dropwisely to a 0.48 M aqueous solution of $Ca(NO_3)_2 \cdot 4H_2O$ (obtained from Sigma–Aldrich, USA) under constant temperature of 70 °C and vigorous stirring. pH of the suspension was adjusted at 10–11 using an aqueous ammonia solution. S-CH precipitate was separated from its suspension by filtration, washed with deionized water then dried at 100 °C for 24 h. Dried powders were further calcined at 800 °C for 1 h, and then finely ground. The average particle size of the ground powder was 4 μm, as determined by scanning electron microscopy.

The two cement-type apatites were prepared in situ using an acid–base reaction between TetCP and DCPA at different molar rations. These apatites had Ca/P molar ratios of 1.6 (abbreviated hereafter as CDS), and 1.5 (abbreviated hereafter as CDH). TetCP was prepared as mentioned elsewhere [8]. In brief, a powder mixture comprising $CaCO_3$ (Osram Sylvania, USA) and MCPM (Sigma, USA) with a molar ratio of 3:1, was heated at 1310 °C for 2 h in air, then quenched to room temperature, producing a phase-pure TetCP powder, as confirmed by X-ray diffraction. TetCP powder was attrition milled to a particle size of 2.5 μm. CDS and CDH precursors were prepared by a mechanochemical process using a powder mixture of TetCP and MCPM, at a Ca/P ratio of 1.6 and 1.5, respectively. All powder mixtures were milled in n-heptane, producing intimate mixtures of TetCP and DCPA with their corresponding Ca/P molar ratios as their starting precursors. Each of these intimate mixtures is known to form its corresponding Ca-def apatite when mixed with deionized water at a powder-to-liquid ratio of 2 [8]. Analytical grade plaster of Paris (POP) was obtained from Sigma–Aldrich, USA, and was used as purchased. Analytical grade gypsum ($CaSO_4 \cdot 2H_2O$, G), also obtained from Sigma–Aldrich, USA, was used for comparison during the characterization of the reaction products.

Powder mixtures of each of the three types of Ca-def apatites were formed by mixing them with POP in weight percentages of 10, 25, 50, and 75 of the apatite. Details of these mixtures and the corresponding samples designations are given in Table 1. Pure samples of POP, CDS, and CDH precursors were used for comparison. An exact weight of 3 g of each of the powder mixtures was mixed with deionized water at a powder: liquid ratio of 2:1 by weight. Heat evolution during the conversion of POP into gypsum in presence of different proportions of each of the three apatites, was recorded for 24 h using an isothermal

Table 1
Details of the starting mixtures and their corresponding samples designations.

Sample details	Ca/P	Method of preparation	Sample designation			
			10%	25%	50%	75%
Pure gypsum[*]	N/A	Cement-type	G100			
Ca-deficient HAp–I	1.6	Cement-type	CDS10	CDS25	CDS50	CDS75
Synthetic Ca-def HAp	1.6	Wet method	S-CH10	S-CH25	S-CH50	S-CH75
Ca-deficient HAp-II	1.5	Cement-type	CDH10	CDH25	CDH50	CDH75

[*] As mentioned in the technical data sheets provided with the product form.

calorimetry (IC) technique (Thermometrics Corp., San Diego, CA, USA). Details of these studies were previously described by Prosen et al. [20]. Aqueous suspensions of each of these mixtures was also formed at a powder-to-liquid ratio of 0.01 to study the variations in their pH with time, for up to 24 h, as a result of conversion of POP into gypsum in presence of each of the apatitic precursors. A calibrated pH electrode interfaced to an Orion 920 pH meter was used in this regard, where each of the powder/water mixtures was placed in a double-walled glass beaker equilibrated at 37.4 °C. At the end of each experiment, the slurry was filtered and the separated solids were flushed with acetone to stop further reactions. After drying, phase composition of each of the filtered solid residues was investigated by X-ray diffraction (XRD) and infrared spectro-scopy (IR) techniques. During each of these experiments, solids were also separated from the suspensions at certain time periods, decided by the IC and pH results, for further detailed characterization by XRD. An automated X-ray diffractometer, with a step size of 0.02°, scan rate of 2° per min, and a scan range from $2\theta = 20°$ to $40°$ was used. A Nicolet Nexus 470 infrared (IR) spectrosphotometer infrared spectroscopy (IR), USA, was used where samples, pre-pressed with KBr, were scanned over the normal range of 4000–400 cm^{-1}. Selected dry solid samples were evaluated for their microstructures using a JEOL SEM at an accelerating voltage of 15 kV.

3. Results and discussion

3.1. Isothermal calorimetric studies

Hydration of POP in the presence of TetCP and DCPA; precursors of CDS and CDH was studied by IC, as shown in Figs. 1 and 2. Martin and Brown [21,22] previously proved that intimate mixtures of TetCP and DCPA proportioned to form calcium-deficient HAp (CD-HAp) through a nucleation-growth

mechanism at a low temperature. Fig. 1 shows the calorimetric curves of those composites originally containing CDS (Ca/P 1.6) and gypsum precursors. In absence of CDS precursors, conversion of POP into gypsum takes place over two steps, shown as two peaks in Fig. 1. The first peak took place immediately after mixing the powder with water at 37.4 °C. Wetting and initial dissolution of the precursors are two events that are known to take place as a result of the first contact between water and the solid particulates. This was followed by a sharp peak with a maxima after 1 h. Normally, dissolution of powders is followed by nucleation then growth, arising as three peaks in their calorimetric graphs. This was found with CDS100 sample, where a nucleation peak was observed after 30 min of the first contact with water, followed by a broad growth peak with a maxima after 1.2 h and ceasing after 12 h of wetting. These findings indicate the relatively faster kinetics of gypsum formation compared with CDS formation in their corresponding pure samples; G100 and CDS100, respectively. It is also evident that a nucleation step could be taking place in a fast fashion that makes it included in the initial wetting/dissolution or growth peaks. Comparing the relative intensities of the wetting/dissolution and growth peaks in G100 with those in CDS100 may indicate that the assumption that a nucleation step is included in the growth peak of the G100 sample due to its relatively faster kinetics, is more acceptable. Fig. 2 also indicates a similar trend where three peaks were noticed during the formation of CDH from its pure precursors. The growth peak in CDH100 sample spans over a time range of 6 h, ceasing after 7.5 h of initial wetting. In the presence of CDS or CDH precursors, the gypsum growth peak was not shown at its normal time; Figs. 1 and 2. Instead nucleation peaks were shown with intensities that decreased with decreasing the concentration of the CDS or CDH precursors in the mixtures. In both sets of samples, mixtures containing 10 wt% of CDS or CDH; CDS10 and CDH10, respectively, showed no nucleation
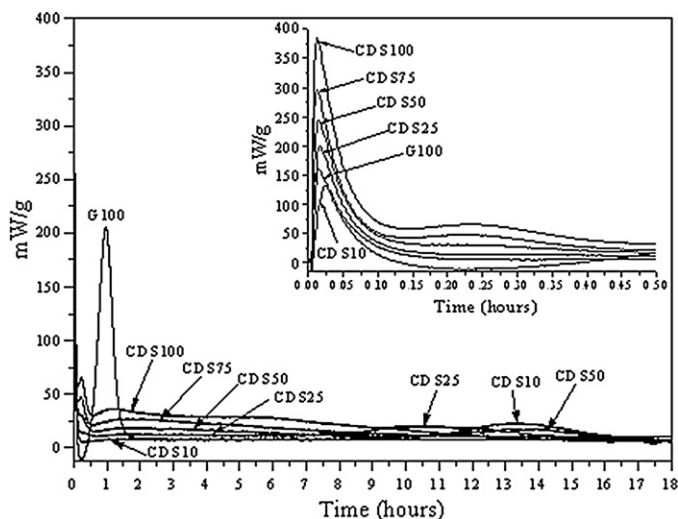

Fig. 1. Calorimetric curves indicating evolution of heat in composites containing gypsum and CDS precursors at weight percentages of 10, 25, 50 and 75 of the later, as a result of their hydration at 37.4 °C for 18 h. Pure CDS100 and G100 are shown for comparison (insert: details of the wetting/initial dissolution peak in all composites within the first 30 min).
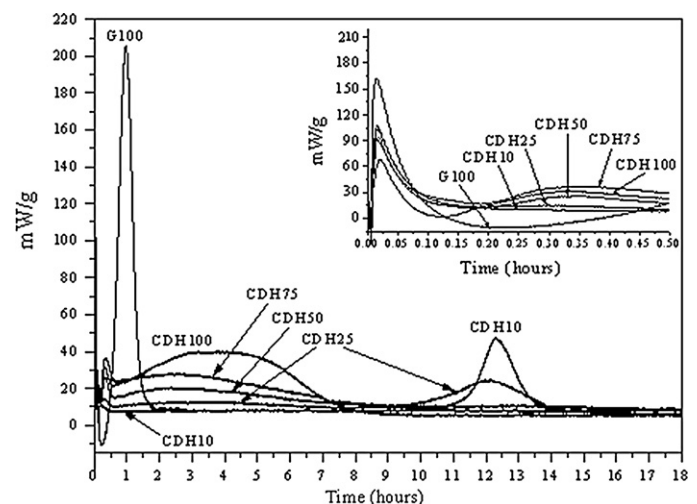

Fig. 2. Calorimetric curves indicating evolution of heat in composites containing gypsum and CDH precursors at weight percentages of 10, 25, 50 and 75 of the later as a result of their hydration at 37.4 °C for 18 h. Pure CDH100 and G100 are shown for comparison (insert: details of the wetting/initial dissolution peak in all composites within the first 30 min).

peaks. Growth peaks, on the other hand, were shown in samples containing 50 and 75 wt% of either CDS or CDH precursors. In addition CDS50 sample showed a second growth peak with a maximum after 13.5 h. This was not observed in CDH50 samples, where a single growth peak with a maximum after 3 h was observed. A low intensity growth peak was observed in CDS25 and CDH25 samples with their major second growth peaks appearing after 10.2 and 12 h, respectively. On the other hand CDS10 and CDH10 samples showed no initial growth peaks, while their major growth peaks appeared with maxima after 13.3 and 12.2 h, respectively. This trend was previously shown in systems containing POP and stoiciometric HAp precursors, where delayed growth peaks were observed in samples containing a majority of POP; S10 and S25, indicating a delayed conversion of POP into gypsum as a result of the presence of calcium phosphate precursors. The presence of two growth peaks in samples containing 50 wt% of the calcium phosphate precursors; CDS, CDH and the previously shown SHAp samples [23], indicates the presence of competing reactions where growth of CDS; CDH or SHAp phases is competing with the growth of gypsum phase.

In contrast, the hydration of POP in the presence of calcined synthetic calcium-deficient HAp with a Ca/P ratio of 1.6 (S-CH) was studied by isothermal calorimetry. Fig. 3 shows the IC curves obtained in this regard. All samples showed initial wetting/dissolution peaks immediately after mixing the powders with water at 37.4 °C. The insert in Fig. 3 indicates a slight variation in the intensity of these initial peaks with the concentration of S-CH in these mixtures. No nucleation peaks were observed in all samples, which is expected due to the fact that a nucleation peak was not observed in G100 samples, and that S-CH was a final product that needed no further reactions to form similar to the CDS/G and CDH/G systems. Instead a pronounced delay and decrease in the intensity of the growth peak of gypsum was observed with increasing the concentration

of S-CH in these mixtures. Maxima of these peaks were observed after 1, 1.7, 3.2, and 3.4 in samples containing 0, 10, 25 and 50 wt% of S-CH, respectively. In contrast, S-CH75 showed a delayed growth peak with a decrease in its intensity after 2.2 h. As was discussed above, the delay in the growth peak of gypsum due to the addition of S-CH could be related to the participation of S-CH in the dissolution/re-precipitation mechanism of gypsum deposition. In a concurrent study, the presence of a synthetic stoichiometric HAp was shown to decrease the intensity of the growth peaks without affecting its time of appearance [23]. Results in Fig. 3 indicate that calcium and phosphate ions released from the relatively more soluble S-CH phase are considered the main reason for the delay in the growth peaks of gypsum in their composites. Fig. 4 shows a study that was carried out to investigate the effect of using S-CH powders, that were thermally treated at different temperatures, on the growth kinetics of gypsum during its formation. Amazingly, the presence of 50 wt% of dry S-CH is shown to accelerate the growth kinetics of gypsum, giving rise to a peak with a maximum within 30 min from the initial wetting with water at 37.4 °C. The presence of calcined or sintered S-CH, on the other hand, is shown to decelerate the growth kinetics of gypsum where the growth peaks appeared with maxima at 2.5 and 7.6 h, respectively. Based on the results of Fig. 3, the participation of S-CH in the growth kinetics of gypsum is, therefore, confirmed. The as-prepared (dry) S-CH was proven more reactive than its calcined and sintered versions, where its dissolution in the aqueous medium seems to be faster than the calcined or sintered versions. The delay in the growth kinetics in the presence of calcined or sintered S-CH could be attributed to the decrease in the reactivity of the S-CH powders as a result of their thermal treatments. In conclusion and based on the above calorimetric results, it is evident that the presence of ready-made Ca-def HAp; S-CH, was shown to affect the growth kinetics of gypsum while maintaining its overall pattern which included the wetting and growth peaks
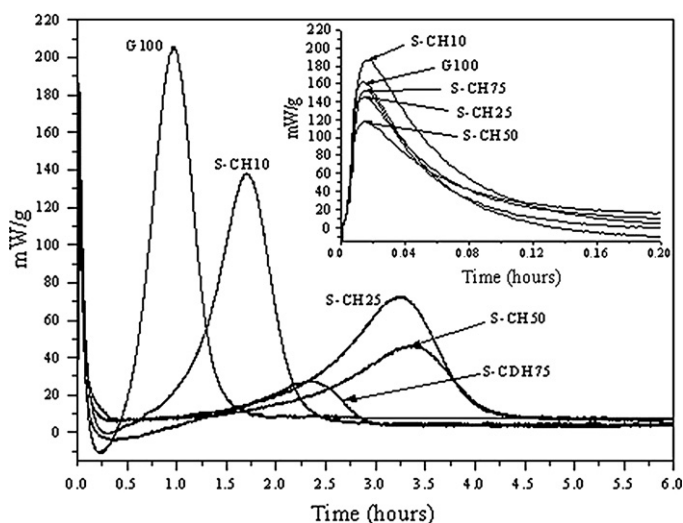

Fig. 3. Calorimetric curves indicating evolution of heat in composites containing gypsum precursors and S-CH powders at weight percentages of 10, 25, 50 and 75 of the later as a result of their hydration at 37.4 °C for 6 h. Pure G100 is shown for comparison (insert: details of the wetting/initial dissolution peak in all composites within the first 15 min).
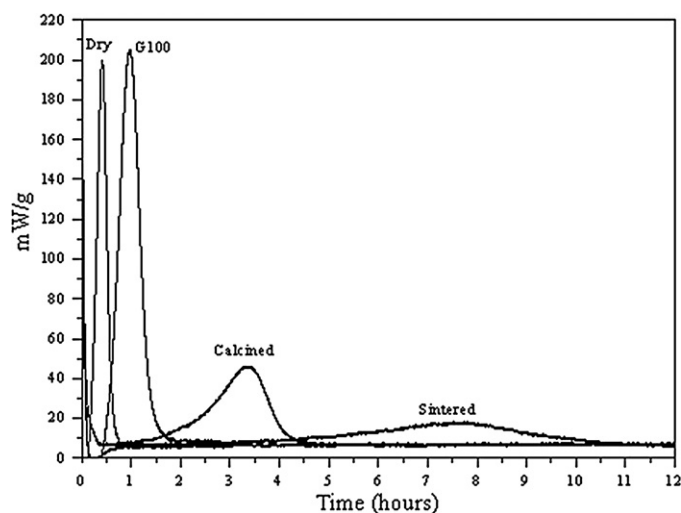

Fig. 4. Calorimetric curves indicating evolution of heat in composites containing gypsum precursors and S-CH powders that were previously dried at 100 °C, calcined at 800 °C/1 h or sintered at 1200 °C/1 h, as a result of their hydration at 37.4 °C for 12 h. Pure G100 is shown for comparison.

only. On the other hand, the presence of precursors that are known to undergo dissolution/re-precipitation process was shown to highly affect the overall kinetics of POP to gypsum conversion. The difference was attributed to the release of more calcium and phosphate ions into the medium through the dissolution of the CDS and CDH precursors, which seemed to be more pronounced than those produced from the relatively less pronounced dissolution of the synthetic S-CH phase.

3.2. pH measurements

Our previous results showed that the acid–base reaction between DCPA and TetCP controlled the pH of the medium depending on the relative proportions of these phases [4,8,22]. A highly alkaline medium was produced when equal molar amounts of TetCP and DCPA were mixed in water, achieving a maximum pH of 10.8 after 6 h of hydration. In the current study, the relative molar proportions of TetCP and DCPA were varied in such a way that Ca-def HAp phases with Ca/P molar rations of 1.5 and 1.6 could be produced. Figs. 5 and 6 show the pH variation as a result of the hydration of pure CDS, CDH and gypsum precursors as well as their composites. In both cases, pH of the medium was shown to increase immediately after the initial wetting of the powders reaching pH values of 9 and 8.2 in solutions containing CDS and CDH precursors, respectively; marked as area I in Figs. 5 and 6. Both showed plateaus that started after 1 h of the initial mixing with water; marked as area II in both graphs. This timing marks the end of the nucleation stage and the beginning of the growth stages that were shown in Figs. 1 and 2. This plateau continued for 4 and 5 h with a slight overall increase reaching its highest values of 9.4 after 6 h and 8.6 after 7 h in solutions containing pure CDS and CDH precursors, respectively. The presence of more TetCP in the CDS precursors' mixture, than that containing CDH precursors, was reflected in an increase in the pH of the solution reaching a maximum of 10.5 after 11 h; within area III in Fig. 5, in contrast to a maximum of 10.8 after 6 h with SHAp precursors. This
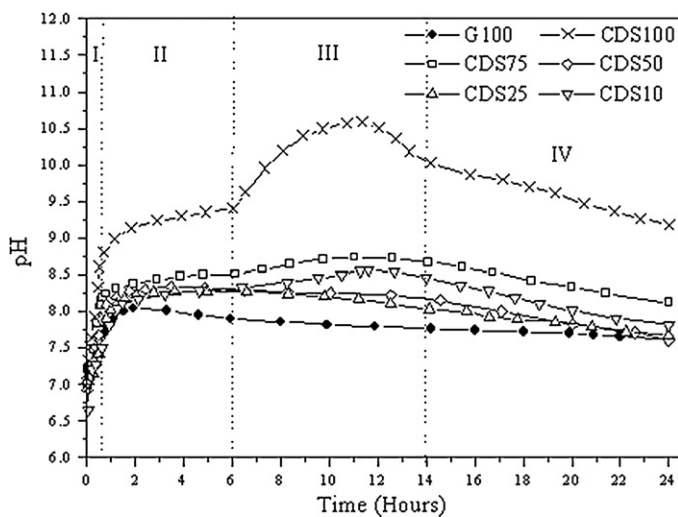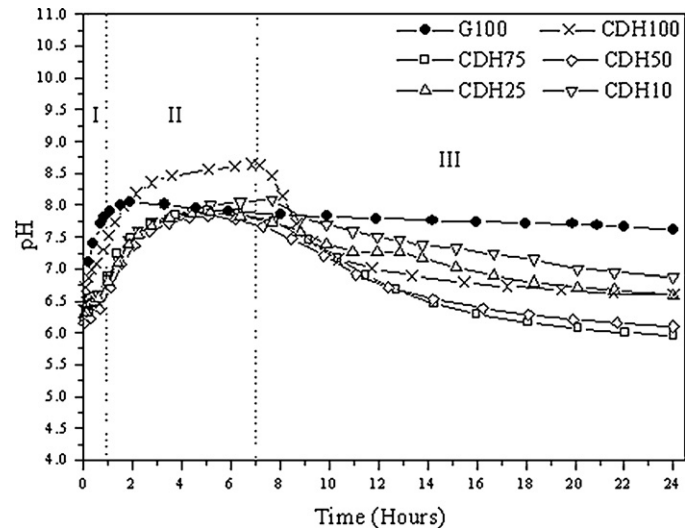

Fig. 6. Variation in pH of suspensions containing gypsum and CDH precursors at weight percentages of 10, 25, 50 and 75 of the later, hydrated for 24 h at 37.4 °C. Pure CDH100 and G100 are shown for comparison.

could be attributed to the presence of lower concentration of TetCP in the CDS precursors' mixture, compared to that in the SHAp precursors' mixture [23]. This was followed by a decrease in the solution pH achieving a value of 9.1 after 24 h; marked as area IV in Fig. 5. On the other hand, the decrease in the pH of the medium containing CDH precursors after 7 h of hydration; within area III in Fig. 6, is an indication that the process was dominated by the more acidic component; DCPA. The lowest pH reached in this regard was 6.6 after 24 h. The inauguration of the pH decrease in both solutions marked the end of the growth peaks shown in Figs. 1 and 2 for pure CDS and CDH samples. This is also related to the consumption of the remaining unreacted precursors; TetCP and DCPA in the CDS and CDH solutions, respectively. Hydration of pure POP, on the other hand, resulted in a sudden increase in the pH of the medium to a maximum value of 8 after 2 h as a result of the dissolution of POP and the subsequent growth of gypsum. By the end of 2 h, which also marked the end of the growth peak previously shown in Figs. 1–3, a slow decrease in the pH of the medium was observed, achieving a minimum value of 7.6 after 24 h of hydration. This is related to the completion of growth of the formed gypsum phase.

An expected pattern of pH variation was expected in solutions containing different proportions of CDS and gypsum precursors where pH of their solutions were less alkaline than that of pure CDS mixture but still slightly more alkaline than that of pure gypsum samples. On the other hand, the presence of more acidic DCPA phase in the composite mixtures containing CDH precursors caused the pH levels of the composite solutions to be lower than that of pure gypsum sample. The delay in the growth kinetics of gypsum in the presence of 10 and 25 wt% of CDS and CDH, previously shown in Figs. 1 and 2, was shown to be highly reflected in the pH behavior of their corresponding solutions. An increase in the pH of CDS10 solution, after 8 h, was shown with a peak of 12.5 h is in accordance with the maximum delayed growth peak observed

Fig. 5. Variation in pH of suspensions containing gypsum and CDS precursors at weight percentages of 10, 25, 50 and 75 of the later, hydrated for 24 h at 37.4 °C. Pure CDS100 and G100 are shown for comparison.
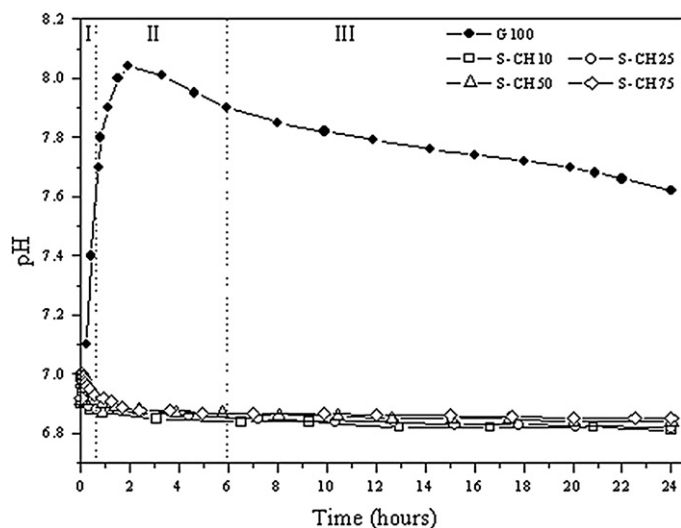
Fig. 7. Variation in pH of suspensions containing gypsum precursors and S-CH powders at weight percentages of 10, 25, 50 and 75 of the later, hydrated for 24 h at 37.4 °C. Pure G100 is shown for comparison.
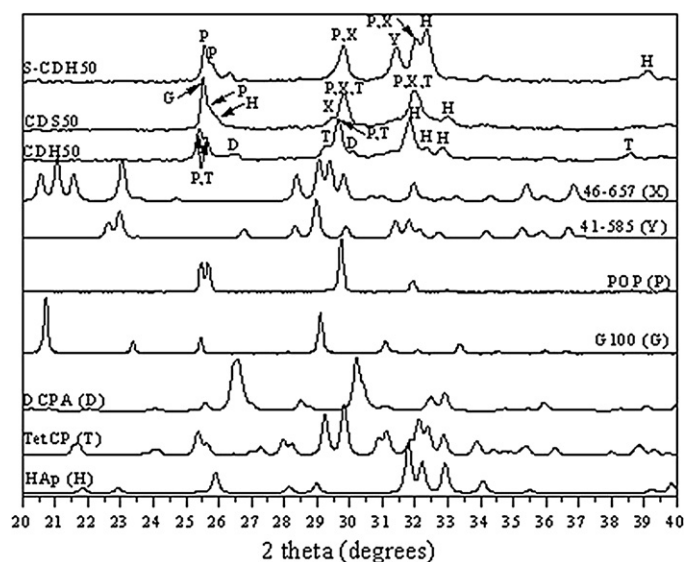

Fig. 8. XRD patterns of composite powders containing 50 wt% of CDS, CDH, and S-CH with gypsum after hydration in deionized water for 6 h at 37.4 °C. XRD pattern of pure POP and G100 samples are shown for comparison. Patterns of standard HAp, TetCP, DCPA and two calcium sulfate phosphate phases are also shown for comparison.

in its corresponding IC curve in Fig. 1. Similarly, the increases in the pH of CDH10 and CDH25 solutions, after 8 h, are in accordance with the appearance of their delayed growth peaks that were previously observed in Fig. 2.

In contrast to the above mentioned observations for the pH variations in solutions containing CDS, CDH and gypsum precursors, variations of pH in solutions containing S-CH and gypsum precursors are shown in Fig. 7. All composites showed an overall lowering in the pH of the composites solutions compared to that of pure gypsum. A closer look at the overall pH ranges obtained revealed a fact that the slight dissolution of S-CH has caused a buffering effect on the solutions, where an almost neutral behavior in all composites solutions was reached. Based on these findings, it could be concluded that the previously observed delay in the growth kinetics of gypsum was attributed to the decrease in the pH of the medium to values below those obtained during the hydration of POP and its conversion to gypsum. A similar trend was previously observed in composite mixtures containing synthetic stoichiometric HAp (S-SH) and gypsum precursors, where a buffering effect was observed as a result of the slower dissolution of the S-SH powders into these solutions [23]. Release of calcium and phosphate ions from the relatively more soluble S-CH, compared to S-SH, is therefore considered the main cause of the delay of the growth kinetics of gypsum in the current system.

3.3. Characterization

Fig. 8 shows the XRD patterns of the solids obtained after 6 h of hydration of composite mixtures containing 50 wt% of CDS, CDH and S-CH precursors. XRD patterns of starting POP and fully hydrated pure gypsum powders were also included in Fig. 8. Standard XRD patterns of pure HAp (9-432), TetCP (25-1137), DCPA (9-80) phases were used for comparison. In addition XRD patterns of two new combined salts are shown. Those are calcium phosphate sulfate hydroxide hydrate

$(Ca_2(SO_4)(HPO_4)\cdot 4H_2O$; Ardealite) (JCPDS card # 41-585) and calcium phosphate sulfate hydrate $(Ca(HPO_4)_x(SO_4)_{1-x}\cdot 2H_2O)$ (JCPDS card # 46-657). The calorimetric curve of CDH50 in Fig. 2 indicated an almost completion of the growth kinetics of the existing phases after 6 h. The XRD pattern of the solid separated after this time showed the presence of HAp at 2θ values of 32.8, 32.4 and 31.8°. The pH curve of this mixture in Fig. 6 shows that this timing is located within the growth plateau where the TetCP and DCPA are still being consumed. This explains the presence of traces of TetCP at 2θ values of 38.7°, 29.3°, 29.7°, 25.6°, 25.4° and DCPA at 26.5°. Peaks at 29.7°, 25.6° and 25.4° may also be attributed to the presence of unreacted POP. Presence of POP can be concluded in this regard based on the fact that gypsum peaks were not observed throughout the XRD pattern of this sample. On the other hand, the incomplete growth of the CDS50 sample, as was previously shown in Fig. 1, was reflected in the presence of the reactant peaks as follows: unreacted TetCP at 32, and possibly at 29.8 °C, unreacted POP possibly at 32°, 29.8° and 25.7°. DCPA was not observed in the XRD pattern of this sample, which confirms the pH findings in Fig. 5 where the alkaline medium was due to the presence of TetCP as the main phase. Signs of the products of the hydration of these composites were also observed, where HAp appeared at 2θ values of 32.9° and 25.9°, while gypsum was shown at a 2θ value of 25.5°. In addition to these phases, those peaks at 2θ values of 31.9 and 29.8 are also closely matching those in the XRD pattern of phase X (card # 46-657) than TetCP or POP. The presence of this double salt was previously shown during the hydration of a composite containing stoichiometric HAp precursors [23], where it was agreed that its formation marked an intermediate step towards the complete deposition of SHAp and gypsum phases. This finding is also valid in the current

CDS50 system and is supported by the fact that the selected timing; 6 h, marked the end of the first growth peak and the beginning of the second growth peak; as shown in Fig. 1.

Although the selected timing; 6 h, marked the completion of the growth kinetics in the S-CH50 sample, the presence of unreacted precursors was shown in the XRD pattern of this sample in Fig. 8. POP was shown at 2θ values of 32°, 29.8°, 25.8°, and 25.6°. HAp was observed at 2θ values of 32.4 and 39.1°. The main peaks of gypsum were not observed in the XRD pattern of this sample, indicating an incomplete conversion of POP into gypsum. It should be mentioned that peaks appeared at 2θ values of 32 and 29.8, which are assigned to POP, are also indicative of the presence of the calcium sulfate phosphate double salt; abbreviated as X on the graph. Moreover, a peak observed at a 2θ value of 31.4° were not matching any corresponding peaks in the starting nor the expected products. The closest match was found with another calcium sulfate phosphate double salt; abbreviated as Y on the graph. The presence of these two types of calcium sulfate phosphate is, therefore, an indicative of the delay of gypsum growth kinetics and the presence of intermediate salts along the pathway of gypsum formation. It should be mentioned that XRD patterns of solids separated after 24 h of hydration revealed the presence of the final products only, where no sign of the starting nor the intermediate phases was found.

Fig. 9 shows the IR spectra of CDS50, CDH50 and S-CH50 together with a phase-pure G100 sample after 6 h of hydration. Standard gypsum phase is characterized by its bands at 601, 669, 1100.9, 1184, 1624.5, 1685.8, 3408.5 and 3548 cm^{-1} [24].
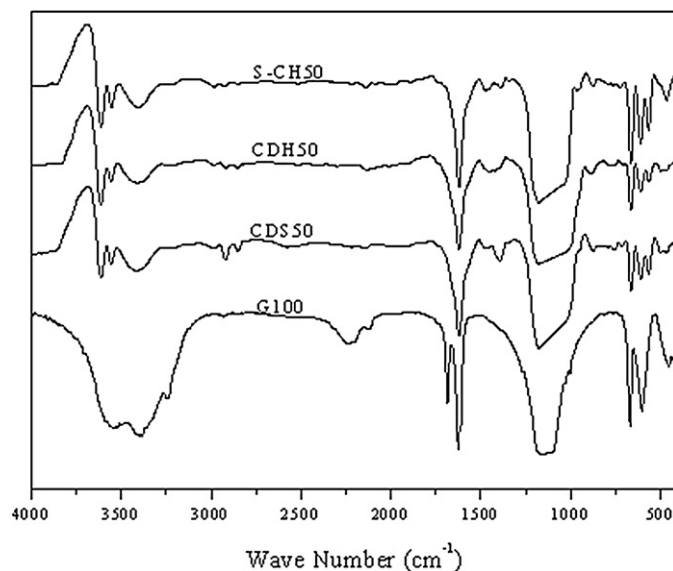

Fig. 9. Infrared spectra of composite powders containing 50 wt% of CDS, CDH, and S-CH with gypsum after hydration in deionized water for 6 h at 37.4 °C. A spectrum of pure gypsum (G100) sample is shown for comparison.

Pure gypsum formed in the current study showed a matched spectrum with the two bands at 1100.9, 1184 cm^{-1} fused in a broad band with maxima extending between 1090.2 and 1190.7 cm^{-1}. The doublet bands at 601.8 and 667.2 and those at 1623.1 and 1685.4; shown in the IR spectrum of pure gypsum, are in close matching with those in the standard sample. Moreover, two more broad bands were observed at 3395.4 and
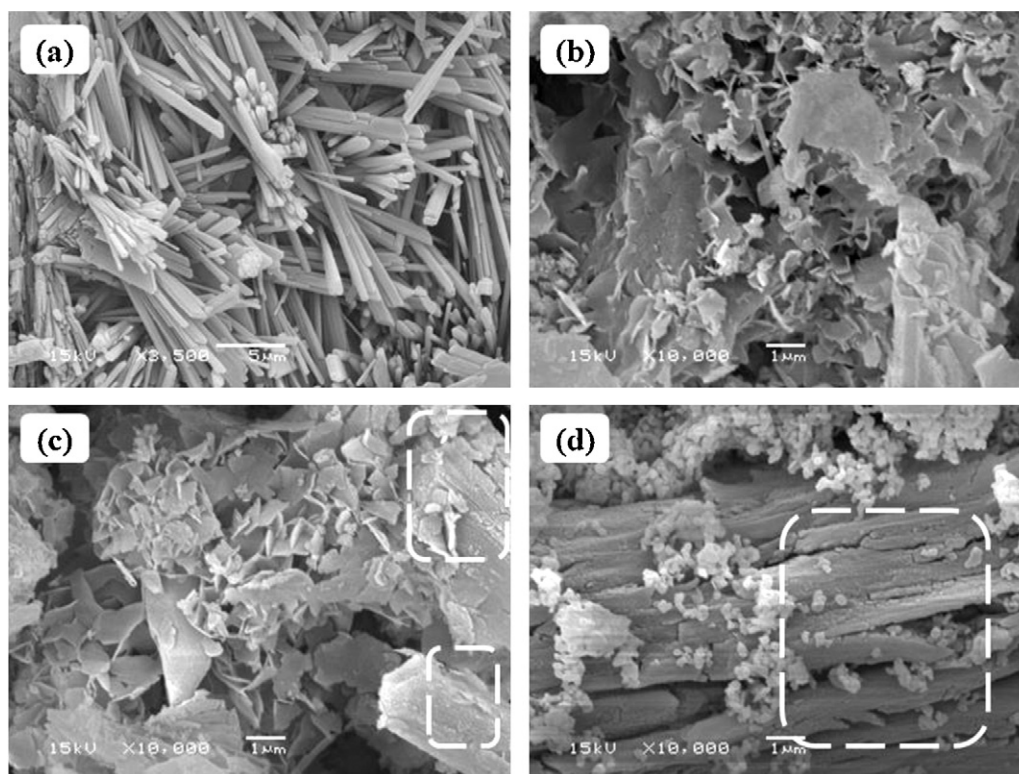

Fig. 10. SEM micrographs of composite powders containing: (a) 0, and 50 wt% of (b) CDS (c) CDH, and (d) S-CH with gypsum after hydration in deionized water for 6 h at 37.4 °C.

3539.6 cm^{-1}, and are closely matching their corresponding bands in the standard sample. In presence of CDS or CDH precursors, broadening of the main band within the range $1090.2–1190.7 \text{ cm}^{-1}$ took place extending its width to be $1009.2–1191.0 \text{ cm}^{-1}$ and $1002.5–1196.9 \text{ cm}^{-1}$. This broadness took place in order to accommodate the apatitic phosphate absorption broad band between 990 and 1104 cm^{-1}. In addition, two more apatitic bands were observed at 567.5 and 611.1 cm^{-1} in the IR spectrum of CDS50 and at 564.4 and 611.1 cm^{-1} in the IR spectrum of CDH50. The disappearance of the gypsum-characteristic band at 1685.4 cm^{-1} in the CDS50 and CDH50 spectra was accompanied with a slight broadening in the band at 1623.1 cm^{-1}. In addition to the gypsum bands at 3395.4 and 3539.6 cm^{-1}, a medium intensity sharp band appeared at 3615 cm^{-1}, which may be attributed to the stretching mode of the apatitic –OH group. A similar pattern was observed in the IR spectrum of S-CH50 solid sample. No evidence of the incomplete growth kinetics in the CDS50, CDH50 or the delayed growth kinetics in the S-CH50 samples was, therefore, observed.

Fig. 10 shows SEM micrographs of the set gypsum cement compared with solid powders collected from suspensions containing 50 wt% of CDS, CDH and S-CH after 6 h of hydration. Gypsum appears in Fig. 10a in its common morphology as elongated needle-shape crystals with homogeneous size distribution and an average fiber size of 15 μm. The micrographs in Fig. 10b and c shows a similar morphology in addition to the typical morphology of Ca-def apatites, appearing as flaky-like crystals with a homogeneous size distribution. Dotted squares on the micrograph in Fig. 10c show the disintegration of a gypsum crystal surface. Compared with those gypsum crystals in Fig. 10a which have smooth surfaces, this indicates that the setting reactions in which POP was converted to gypsum in the presence of calcium phosphate precursors took place via a different delayed fashion in which deformation of the gypsum crystals took place. This was further confirmed in the micrograph of S-CH50 in Fig. 10c, and is highlighted by a dotted square. As a common feature, all micrographs revealed the porous nature of the composites and the interlocking between the deposited Ca-def apatite flakes and the gypsum crystals.

4. Conclusions

The current study investigated the effect of presence of bioresorbable Ca-def apatites, with different origins, on the growth kinetics of gypsum during the formation of their corresponding composites. Two cement-type Ca-def apatites and a synthetic type were investigated. Results revealed the effect of the release of calcium and phosphate ions from the CDS and CDH precursors, during the process of dissolution of their precursors and the consequent precipitation of these phases, on the growth kinetics of gypsum. A remarkable delay

on the growth kinetics of gypsum as observed in both cases, with different extents depending on the starting Ca/P molar ratios of the apatite and its proportion in the composites. The bioresorbability of the synthetic version of Ca-def apatite also revealed its retardation effect on the formation of gypsum. An overall near physiologic pH regimes were obtained by combining POP with each of the Ca-def apatites in their solutions. Phase composition of the formed composites confirmed the retardation effect on the growth kinetics of gypsum. Taken together, these results show that novel bone cements could be prepared using bioresorbable apatite and gypsum precursors. Optimization of the setting reactions of gypsum in presence of these different apatites is currently under investigation, and is dictated by the characteristics of the formed cements.

References

[1] J.C. Elliot, Structure and Chemistry of the Apatites and Other Calcium Orthophosphates, Elsevier, Amsterdam, 1994.
[2] R.Z. Legeros, Calcium Phosphates in Oral Biology and Medicine, Karger, Basel, 1991.
[3] R.I. Martin, P.W. Brown, J. Biomed. Mater. Res. 35 (1997) 299.
[4] W.E. Brown, L.C. Chow, A New Calcium Phosphate, Water-setting Cement, American Ceramic Society, Westerville, 1987.
[5] B. Flautre, J. Lemâitre, C. Maynou, P. Van Landuyt, P. Hardouin, J. Biomed. Mater. Res. 66A (2003) 214–223.
[6] M. Ikenaga, P. Hardouin, J. Lemâitre, H. Andrianjatovo, B. Flautre, J. Biomed. Mater. Res. 40 (1998) 139–144.
[7] H. Monma, T. Kanazawa, J. Ceram. Soc. Jpn. 108 (2000), S75- S80.
[8] Y. Greish, P. Brown, J. Biomed. Mater. Res. Part B: Appl. Biomater. 67B (2003) 632–637.
[9] G. Orsini, J. Ricci, A. Scarano, G. Pecora, G. Petrone, G. Lezzi, J. Biomed. Mater. Res. Part B: Appl. Biomater. 68B (2004) 199–208.
[10] P. Maragos, N.F. Bissada, R. Wang, R.P. Cole., Int. J. Periodont. Restor. Dent. 22 (2002) 493–501.
[11] Y.E. Greish, Egyp. J. Chem. 22 (2007) 2728–2734.
[12] J. Lemâitre, E. Munting, A. Mirtchi, Stomato 91 (1991) 1–5.
[13] E. Fernández, M. Vlad, M. Gel, J. López, R. Torres, J. Cauich, M. Bohner, Biomaterials 26 (2005) 3395–3404.
[14] M. Nilsson, E. Fernandez, S. Sarda, L. Lidgren, J.A. Planell, J. Biomed. Mater. Res. 68B (2002) 199–208.
[15] M. Bohner, Biomaterials 61 (2004) 600–607.
[16] C.K. Kim, H.Y. Kim, J.K. Chai, K.S. Cho, I.S. Moon, S.H. Choi, J.S. Sottosanti, U.M. Wikesjo, J. Periodont. 69 (1998) 982–988.
[17] G.E. Pexcora, D. DeLeonardis, C.D. Rocca, R. Cornelini, C. Cortesini, Int. J. Oral Maxillo. Imp. 13 (1998) 866–873.
[18] M.H. Bai, X.Y. Liu, B.F. Ge, C. Yallg, D.A. Chen., Int. Surg. 81 (1996) 390–392.
[19] S. Sato, T. Koshino, T. Saito, Biomaterials 19 (1998) 1895–1900.
[20] E.J. Prosen, P.W. Brwon, F.L. Davies, Cem. Concr. Res. 15 (1985) 703.
[21] R.I. Martin, P.W. Brown, Aqueous formation of hydroxyapatite, J. Biomed. Mater. Res. 35 (1997) 299–308.
[22] P.W. Brown, J. Am. Ceram. Soc. 75 (1992) 17–22.
[23] Y.E. Greish, phase evolution during the low temperature formation of stoichiometric hydroxyapatite–gypsum composites, Ceram. Int. 37 (2011) 715–723.
[24] J.A. Gadsden, Infrared Spectra of Minerals and Related Inorganic Compounds, Butterworth Group, USA, 1975.